ISSN: 2642-1747

# **Case reports**

Copyright© Trainini Jorge

# The Three Electromechanical Units of the Myocardium

Trainini Jorge<sup>1\*</sup>, Beraudo Mario<sup>2</sup>, Wernicke Mario<sup>2</sup>, Trainini Alejandro<sup>3</sup>, Elencwajg Benjamín<sup>3</sup>, Lowenstein Jorge<sup>4</sup>, Herrero Efraín<sup>5</sup>, Cohen Marta<sup>6</sup> and Carreras Costa F<sup>7</sup>

<sup>1</sup>Presidente Perón Hospital, National University of Avellaneda, Argentina

<sup>2</sup>Güemes Clinic, Luján, Argentina

<sup>3</sup>Presidente Perón Hospital, Avellaneda, Argentina

<sup>4</sup>Diagnostic Institute of Medical Research, Buenos Aires, Argentina

<sup>5</sup>Henderson Hospital, Pcia. de Buenos Aires, Argentina

<sup>6</sup>Histopathology, Sheffield Children's NHS Foundation Trust, United Kingdom

<sup>7</sup>Co-Director of the Cardiac Imaging Unit, Creu Blanca Clinic, Barcelona, Spain. Honorary Director of the Cardiac Imaging Unit, Hospital de la Santa Creu i Sant Pau, Barcelona

\*Corresponding author: Jorge Carlos Trainini, Presidente Perón Hospital, National University of Avellaneda, Argentina.

To Cite This Article: Trainini Jorge\*, The Three Electromechanical Units of the Myocardium. Am J Biomed Sci & Res. 2025 29(1) AJBSR. MS.ID.003760, DOI: 10.34297/AJBSR.2025.29.003760

Received: 

☐ October 14, 2025; Published: 
☐ November 10, 2025

#### **Abstract**

During this investigation, in both human, bovine and porcine hearts, the histological study revealed that the fulcrum (myocardial support, the beginning and end of the continuous myocardium) is adjacent to the AV node, creating a space rich in neurofilament plexuses. A crucial finding is that neurofilaments also occupy the cardiac fulcrum, constituting an electromechanical unit. This contiguity between the two structures is found in all specimens studied, both in bovine, porcine and human hearts. Central to the research finding is that neurofilaments are also found within the cardiac fulcrum. Fibroblasts and connective tissue are located in the thickness of the conduction system and between this and the working myocardium, acting as an insulation layer. It is also the connective tissue that constitutes the fibrous ring and the central fibrocartilaginous portion of the fulcrum, thus electrically isolating the atrial and ventricular chambers.

We mapped left ventricular activation on its endocavitary and epicardial surfaces according to the methodology described above. The mapping was performed simultaneously with the surface ECG. This provided a unified temporal reference frame, allowing both recordings to be correlated and, on the one hand, to obtain a synchronized view of the simultaneous activation observed in various electroanatomical incidents. This study found a relationship between myocardial stimulation and its mechanical product. The mechanical consequence of the cardiac structure is the initiation of stimulation in the anatomical and functional unit between the AV node and the cardiac fulcrum, and its continuity in myocardial activation up to the simultaneous activation zone with opposite movements between the descending and ascending segments, which generates torsion of the myocardium, due to opposite rotation between the base and the apex, with simultaneous shortening of both ventricles.

In summary, cardiac movements are governed by three units: 1) Energy unit, constituted by the AV node; 2) Electromechanical unit, located at the cardiac fulcrum where the neurofilaments interact with the myocardium; 3) Torsion/detorsion unit, this occurs at the level where energy is transferred from the descending segment to the ascending segment, achieving myocardial torsion (systole) and the subsequent detorsion that allows ventricular suction.

Keywords: Myocardial torsion, Cardiac activation, Cardiac fulcrum, AV node



#### Introduction

The complexity of biological phenomena implies dynamism, progression, and the simultaneous coexistence of various stages and different structures within an organizational unit. The same occurs in the heart from the perspective of electrical, mechanical, and electromechanical phenomena, with myocardial activation, contraction, and relaxation during systole, suction, and diastole. Although various aspects of electrical stimulus propagation through the ventricles have long been known, the advent of three-dimensional navigators and electroanatomical mapping has allowed for a much more detailed study of the same in the human heart in completely physiological clinical situations.

There is always an opportunity in nature where functions beyond those known can be integrated with the components that make up a system [1,2]. This is the case of the "pulse center." The heart has historically been studied in its participating components, with a global and homogeneous contraction, simultaneous throughout its entire muscular structure; but not with a clear understanding that the movements in its different phases occur sequentially and overlap, contributing to its function in a complex manner with a tiny time of less than one second per cycle and 100,000 cycles per day. The heart has been studied only partially, surely because relating the complexity of its function to the duration of its cycle implies the difficulty of observing the reality that happens to it.

This situation was noted by William Harvey (1578-1657), who recounts the difficulties in proving his theory of blood circulation: "I came to think, [he says] with Fracastoro, [Renaissance epidemiologist], that the movement of the heart could only be known by God". Due to the rapidity of cardiac movement, Girolamo Fracastoro (Verona, 1478-1553) had expressed this concept in his book "De sympathía et antipathía rerum" (Venezia, 1546) [3]. It is understandable to consider that the integrity proposed by the general theory of systems will remain relegated as long as adherence to solely analytical models continue, reducing the whole to the sole study of its parts. Through the development of technology applied to morphology, a comprehensive biological perspective adapted to functional requirements was achieved [4-8]. This view of the cardiac organ and its function that we have investigated is in line with general systems theory [9-11], a situation that we consider throughout our research.

Our previous publications corresponding to the cardiac fulcrum as a support for the myocardium, its relationship with the Aschoff-Tawara node and the sequential activation of the heart in a clear organizational arrangement to achieve the torsion movement [12-18], led us to analyze these structures in terms of their potential and functional aspects [10-23]. In this way, we arrived at the concept that the myocardium acts through three fundamental units, which include: activation, electromechanical unit and torsion, which are interrelated in their anatomy and organization to be able to act in accordance with a highly efficient system.

This study analyzed the anatomical and histological relationship between the cardiac fulcrum and the atrioventricular node in human, porcine, and bovine hearts, as well as the myocardial activation channels that cause cardiac torsion and detorsion. The methods used to explain the hypothesis of the anatomical and functional integrity of the heart consisted of:

- 1. The use of 87 hearts from morgues, slaughterhouses, and breeding farms (for anurans):
- a) 56 two-year-old bovines weighing between 1300 and 1900 g (average 1650 g)
- b) 17 humans (three at 8, 16, and 23 weeks of gestation, respectively; four infants at 30 days, 36 days, 10 weeks, and 27 weeks; one 4-year-old child; one 10-year-old child; and eight adults with an average weight of 300 g)
- c) 4 porcine (400 g)
- d) 10 anurans
- 2. Histological and histochemical analysis of anatomical samples.
- 3. Endo- and epicardial electrical activation of the left ventricle in humans using three-dimensional electroanatomical mapping.

In the research results, we find the reference points required to present an organizational pattern that contributes to cardiac function. These are: the anatomical contiguity between the AV node and the cardiac fulcrum; the continuous presence of the filaments that structure the AV node within the fulcrum-where the myocardium begins-clearly interpreting the formation of an electromechanical unit; and the activation pathway through the myocardium that allows for helical torsion, through the anatomical, anisotropic, and functional spatial location between the descending and ascending segments at the septal level, confirmed by ultrasound and electrophysiological studies. At this point we must analyze how these elements interact, including energy and mechanical transfer structures and circuits. The analysis closely corresponds to myocardial movements and the stimulation that runs through its segments, according to the electrophysiological studies we have performed. The interpretation of the anatomical relationships between the cardiac fulcrum and the AV node implies the complementarity of anatomy with the physiology of the continuous helical myocardium, since the contiguity they exhibit is located at the site where stimulation begins and ends, producing the mechanical action of torsion and detorsion in the systolic and suction phases of the ventricles as the different myocardial segments are activated.

#### **Cardiac Electrical Activation**

The left ventricular endo and epicardial electrical activation sequence was studied using three-dimensional Electroanatomic Mapping (3D-EAM) with Carto navigation and mapping system (Bi-

osense Webster, California, USA), enabling three-dimensional anatomical representation, with electrical activation and propagation maps. Isochronic and activation sequence maps were performed, correlating them with surface ECG. Also, endocardial and epicardial ventricular activation maps were made, achieving detailed high-density recordings in apical, lateral and basal views. The study

was performed at Hospital Presidente Perón (Buenos Aires, Argentina), including patients who had signed an informed consent. The research was previously approved by the Institutional Ethics Committee. All patients were in sinus rhythm, with normal QRS and had no verifiable structural cardiac disease by Doppler echocardiography and resting and stress gamma camera studies (Table 1).

Table 1: Patient characteristics.

Patient	Age (years)	Gender	Study indication	Other diseases
1	42	F	Isolated atrial fibrillation	NO
2	19	М	Abnormal left epicardial pathway	NO
3	23	М	Abnormal left epicardial pathway	NO
4	29	М	Abnormal left epicardial pathway	NO
5	32	М	Abnormal left epicardial pathway	NO

The 3D-EAM was performed during the course of radiofrequency ablation for arrhythmias owing to probable abnormal occult epicardial pathways. Mapping was carried out at the onset of studies, followed by ablation maneuvers. No complications developed. The presence of abnormal pathways did not interfere with mapping, as during the whole procedure baseline sinus rhythm was preserved with normal QRS complexes, both in duration and morphology, without antegrade preexcitation. As the muscular structure of the left ventricle is made up of an endocardial layer (descending segment) and an epicardial layer (left and ascending segments), two

approaches were used to carry out the mapping. Endocardial access was performed through a conventional atrial transseptal puncture. The epicardial access was obtained by means of a percutaneous approach in the pericardial cavity with an ablation catheter [24]. The endo and epicardial mappings were performed consecutively and immediately and were later superimposed, synchronizing them by electrocardiographic timing. Thus, a simultaneous mapping of both surfaces was obtained, with the propagation times of electrical activation through the myocardium measured in milliseconds (ms) (Figure 1).



Note\*: 1: Catheter located in the right atrium; 2: Endocavitary catheter; 3: Catheter in the pericardial space.

Figure 1: Epicardial mapping.

Up to that moment, the theory of the continuous myocardium lacked a fundamental investigation, as there was no documentation on the electrophysiological mechanism supporting the mechanical activation sequence of the helical anatomical model. The advent of clinical 3D-EAM overcame that limitation, as it not only allows the independent recording of different ventricular areas but also of exclusive or integrated endocardial and epicardial areas. We performed a left ventricular activation mapping of its endocavitary and epicardial surfaces, according to the methodology described above. Mapping was carried out simultaneously with surface ECG, providing a unified temporal reference framework that enabled on the one hand the correlation of both recordings and on the other the synchronized view of the simultaneous activation observed in different electroanatomical conditions.

As 3D-EAM corresponded to the left ventricle, the activation wave previously generated in the right ventricle was not obtained.

Three-dimensional electroanatomical mapping lasted approximately 20 minutes. There were no complications associated with the procedure or any of the accesses. Figures 2 to 5 show the propagation of endocardial an epicardial electrical activation. In all the figures the right projection is observed in the left panel and the simultaneous left anterior oblique projection in the right panel. At each time, the activated zones are detailed in red. The lateral inset represents the activation of the descending and ascending muscle bands that make up the ventricular continuous structure of the myocardium in the cord model, a simplification of the three-dimensional myocardial spatial structure. In all figures, the area depolarized at that time is represented in red and those that were previously activated and are in refractory period are represented in blue. Below the cord model, the average electrical propagation time along the myocardium can be seen measured in milliseconds (ms) at the analyzed site (Tables 2 and 3).

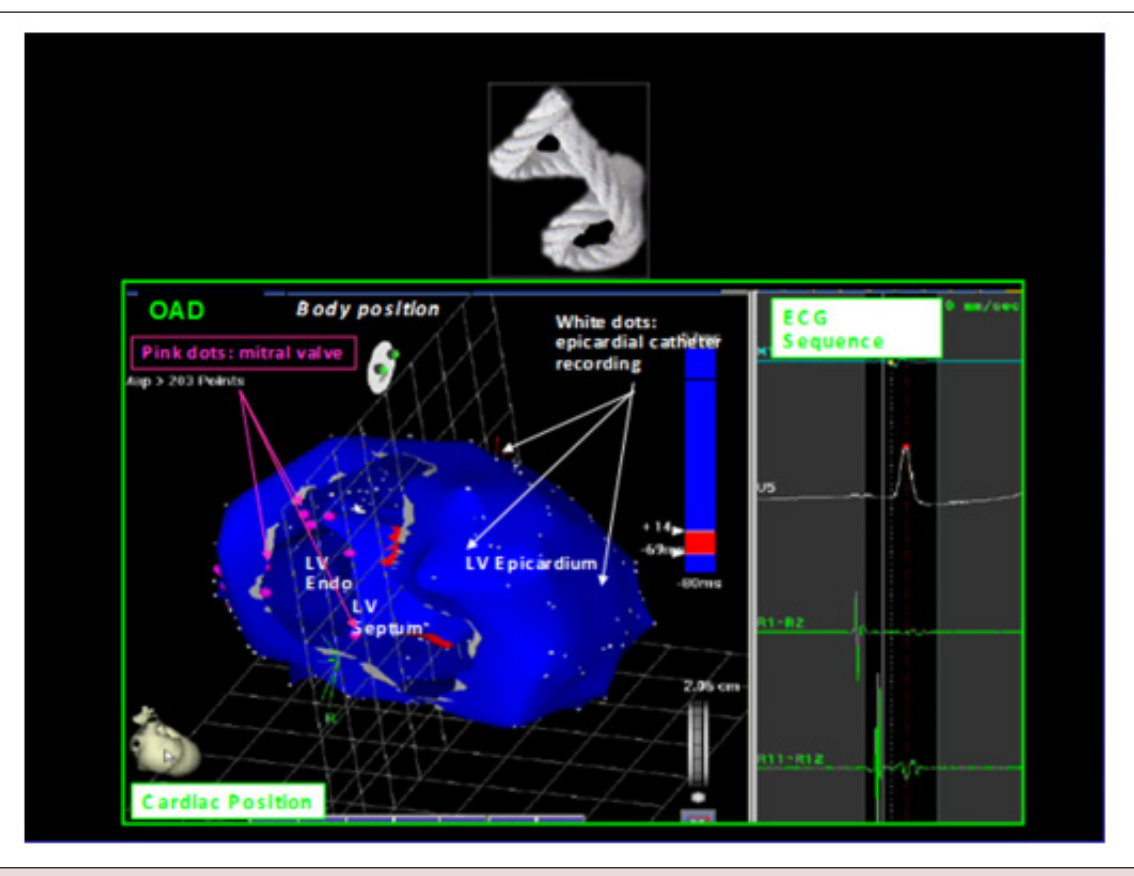


Figure 2: Integrated endo-epicardial mapping. The left panel shows the mitral valve annulus (limited by pink dots), the Left Ventricular (LV) endocardium, the LV septal endocardium and the LV epicardium. The blue vertical bar to the right of the panel indicates total cycle duration and the red zone within it, the activation moment corresponding to the activation graph on the left. The right panel shows the surface ECG. The red dot at peak QRS indicates the point of gated trigger. The green channels correspond to reference electrograms. The dotted vertical line shows QRS onset and the full line the present recording moment. The upper panel represents Torrent Guasp's cord model.

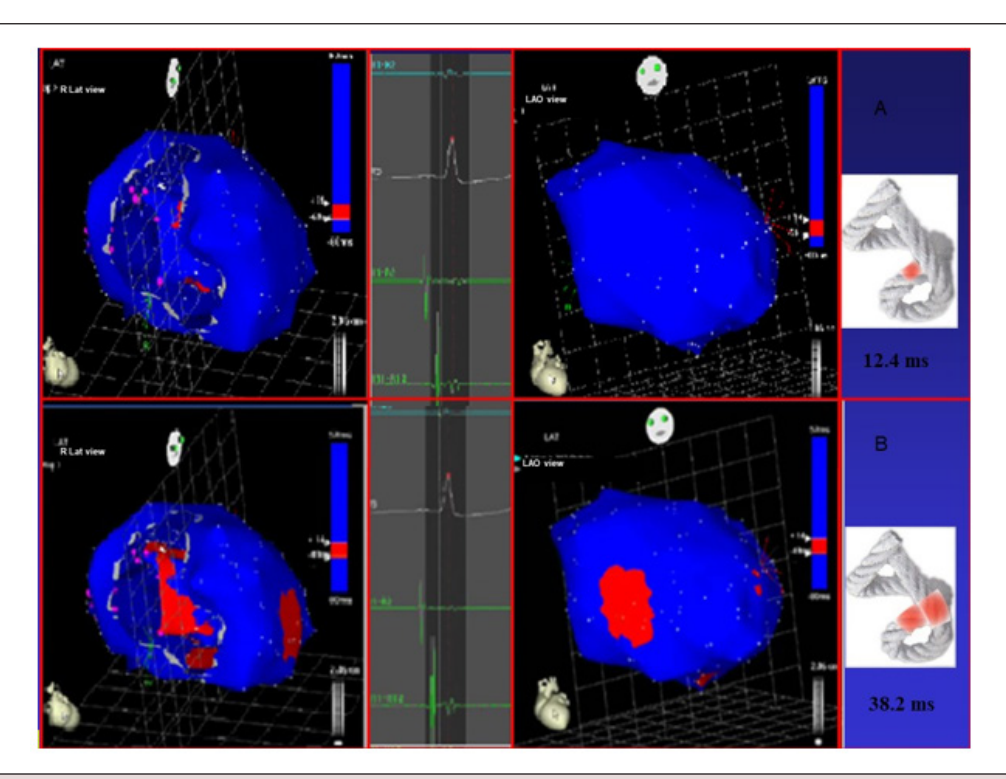
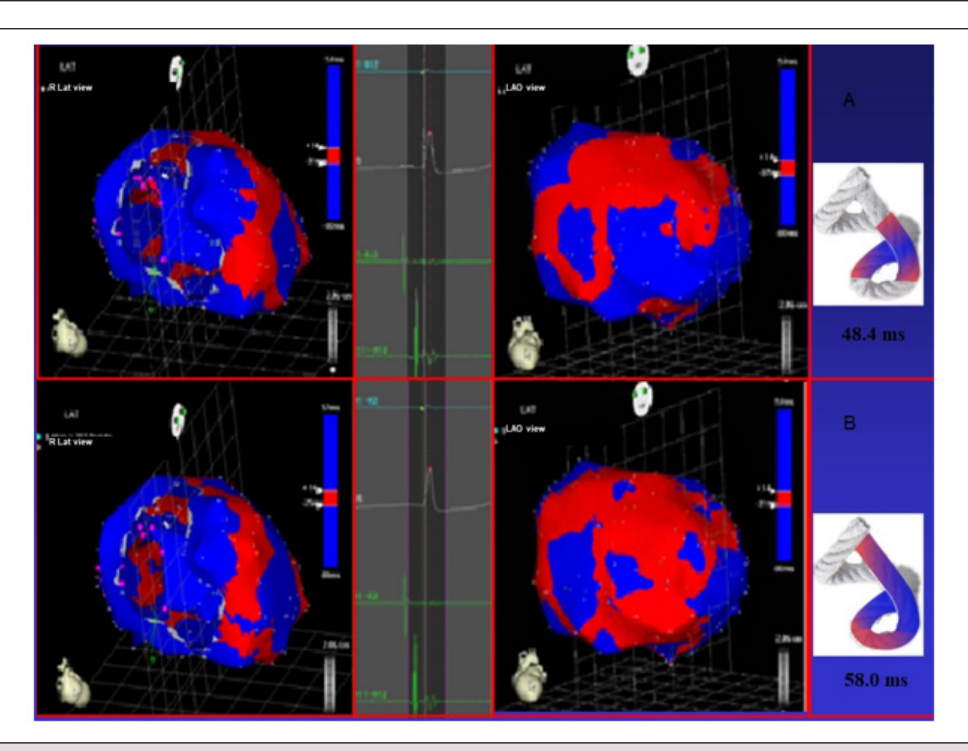
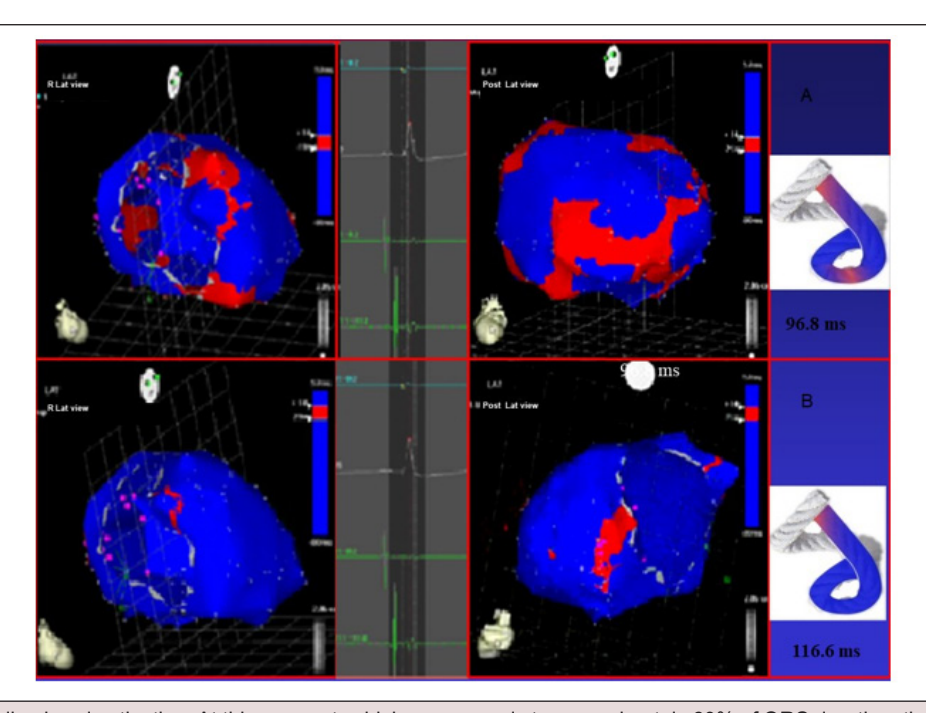


Figure 3: A: Onset of left ventricular activation. The left panel shows interventricular septum depolarization, corresponding to the descending band. In the right panel, the ventricular epicardium (ascending band), which has not been activated yet. B: Simultaneous band activation. Activation progresses in the left ventricular septum through the descending band (longitudinal activation) and propagates simultaneously to the epicardium (transverse activation) activating the ascending band.



**Figure 4:** A: Bidirectional apex and ascending band activation. The final activation of the septum is observed, progressing towards the apex, synchronously with the epicardial activation in the same direction. At the same time the epicardial activation is directed towards the base of the left ventricle. B: Activation progression. Activation progresses in the same directions of the previous figure.



**Figure 5:** A: Late ascending band activation. At this moment, which corresponds to approximately 60% of QRS duration, the intracavitary activation (descending band) has already been completed. The distal portion of the ascending (epicardial) band is depolarized later. This phenomenon correlates with the persistence of this bands's contraction in the initial phase of diastole. B: Final activation. In the right panel, the left anterior oblique projection was modified to a left posterolateral projection, evidencing the very late activation of the distal portion of the ascending band.

Left ventricular activation occurs 12.4 ms±1.816 ms after the onset in the interventricular septum (Figure 3 A). This contraction is determined by the bundle of His and its conduction fibres that give origin to the Purkinje network. Based on the anatomy that these fibers occupy, the endocardium is the first area of the left ventricle to receive electromechanical activation. At that moment it also propagates to an epicardial area - ascending band- evidencing a transverse activation at a point we call "band crossover" which is produced 25.8±1.483ms after septal stimulation (Figure 3 B, Table 3) and at 38.2±2.135 ms from the onset of cardiac activation.

This leads to subendocardial shortening and subepicardial lengthening, resulting in opposite rotations between the ventricular base (counterclockwise) and apex (clockwise). In echocardiographic studies verifying stimulation-function at this time of the cardiac cycle, greater systolic torsion was found in the mid-interventricular septum than in the anterior walls. Synchronously, following the anatomical arrangement of the descending band, the activation propagates longitudinally towards the ventricular apex, reaching it at 58±2.0 ms (Figures 4 A and B, Table 2).

Table 2: Activation times of the different cardiac structures (ms) (See explanation in the text of the cited figures).

Site	Patient 1	Patient 2	Patient 3	Patient 4	Patient 5	X	SD
Figure 3 A	10	12	13	15	12	12.4	1.816
Figure 3 B	35	38	37	41	40	38.2	2.135
Figure 4 A	45	47	49	52	49	48.4	2.332
Figure 4 B	55	59	57	61	58	58	2
Figure 5 A	94	98	98	99	95	96.8	1.939
Figure 5 B	115	118	114	120	116	116.6	2.154

Note\*: ms: milliseconds; X: Mean; SD: Standard deviation.

Table 3: Radial propagation time (ms).

Time	Pat.1	Pat.2	Pat. 3	Pat. 4	Pat. 5	X	SD
Radial time from descending to ascending band	25	26	24	26	28	25.8	1.483

Note\*: Patient; ms: milliseconds; X: Mean; SD: Standard deviation.

From "band crossover" onwards the activation loses its unidirectional character and becomes slightly more complex. Three simultaneous wave fronts are generated: 1) the distal activation of the descending band towards the apical loop, 2) the depolarization of the ascending band from band crossover towards the apex and 3) the activation of this band from the crossover point towards its final portion in its insertion in the cardiac fulcrum, myocardial support. Figures 4 B, 5 A and B show the continuation and completion of this process. Intracavitary activation ends long before QRS termination

(Figure 5). The rest of the QRS corresponds to the late activation of the distal portion of the ascending band, which justifies the persistence of its contraction during the isovolumic diastolic phase. This contraction constitutes the basis of the ventricular suction mechanism (Figure 5), and for this reason, it will be now termed Left Ventricular Protodiastolic Phase of Myocardial Contraction (LVP-PMC), as in it there is contraction and no relaxation. A synthesis of the stimulation found in this study is shown with the cord model in Figure 6.

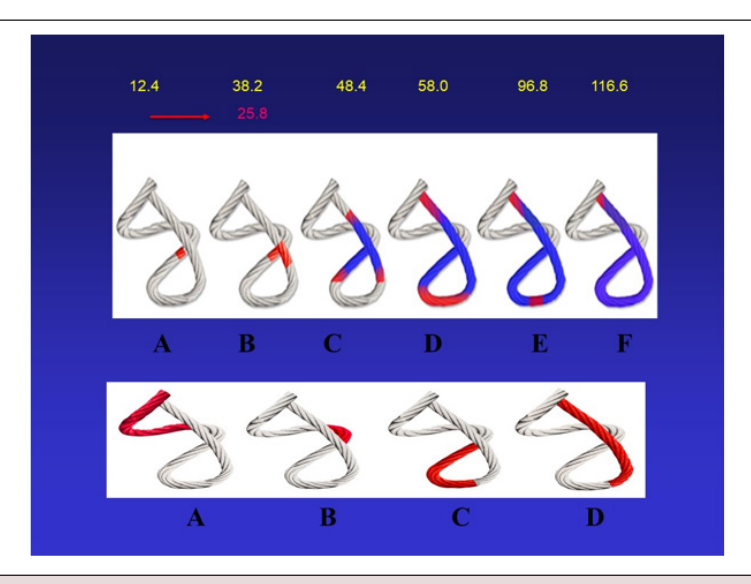


**Figure 6:** Cord model. Upper panel: Activation Sequence (A-F) in the continuous myocardium according to our investigation. The figure shows the propagation times. The 25.8 milliseconds in B indicate the delay in the stimulation to pass from the descending band in A to the ascending band in B. References: In red: depolarization; in blue: already activated zones. Lower panel: unidirectional excitation propagation (in red) in the continuous myocardium according to Torrent Guasp's theory (A-D).

The right ventricle initiates its systolic activity, in our research, 12.4 ms before the left ventricle. The opening of the pulmonary valve begins as soon as its intraventricular pressure rises to 8-10mm Hg. The right ventricular inflow tract contracts very early. This onset of right ventricular ejection precedes left ventricular systole. Only at an average of 38.2 ms in our research, after the beginning of the cardiac cycle with right ventricular contraction, are the ascending and descending segments stimulated, which would imply left ventricular ejection at that moment when the aortic valve opens. This difference between the early opening of the pulmonary valve relative to the aortic valve of 40 ms is logical, since with both ventricles ejecting and filling simultaneously, circulation would be practically interrupted, lacking the necessary continuity, falling to levels even lower than the gradients exhibited by normal circulatory return.

The two active functions of ejection and suction, synchronized between both ventricles, would correspond to circulatory continuity. This raises the question: how is the early opening of the pulmonary valve relative to the aortic valve based? The ventricles take advantage of the asynchronous impulse of approximately 40 ms, or 5% of the 800 ms duration of the cardiac cycle, so that one of them, the right ventricle, collaborates in the loading of the other, the left, through the complementarity between ejection and suction. Correlating this early opening of approximately 40 ms of the

pulmonary valve relative to the aortic valve found in our research in humans, the same has also been observed in fish. Thus, in teleosts (Cretaceous period), which have four cardiac chambers in line (sinus venosus, atrium, ventricle and bulbus arteriosus), the same delay of 40 ms has been found in the deflection of the myocardium after the discharge of the spike, between the proximal and distal ventricle at the level of the bulb, analogous to the right and left ventricles of mammals (Figure 7) [6,25]. This correlation implies an evolutionary biological matrix that transcends species. In this estimated interval of at least 38.2 ms on average in our investigations, between the openings of the pulmonary valve and the aortic valve, the last phase of filling of this ventricle occurs in the left ventricle (diastolic period 3).

## **Myocardial Torsion**

As noted, left ventricular activation begins in the endocardial descending band, which is depolarized longitudinally and transversally almost simultaneously. At the crossover point of both bands, the activation propagates from the endocardium to the epicardium (transverse propagation), that is, from the descending to the ascending band. From this point onwards, the ascending band depolarizes in two directions: towards the apex and towards the base, at the same time that the descending band completes its activation towards the apex (Figure 4). Thus, two essential phenomena occur:

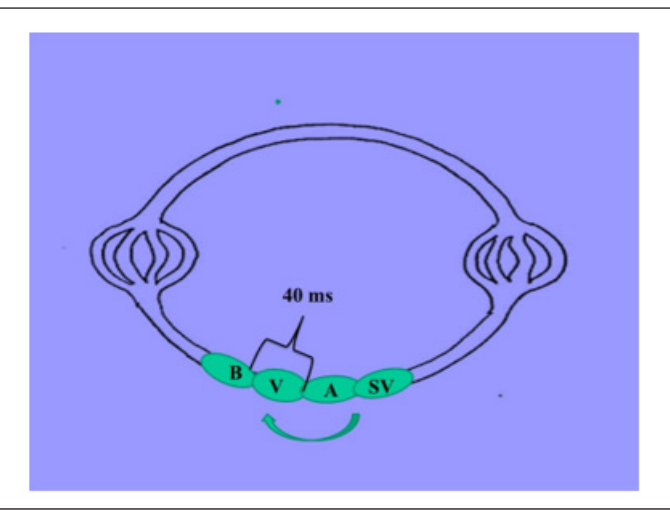


Figure 7: The diagram of the circulatory system of a teleost fish shows the delay in obtaining myocardial deflection from the proximal ventricle (right ventricle) to the distal and bulbus (left ventricle). This 40 ms time is analogous to what we found in our electrophysiological research in humans between the opening of the pulmonary valve and the aortic valve. The diagram represents the cardiac chambers of a teleost fish, which are located in a line: Sinus Venosus (SV), Atrium (A), Ventricle (V), and Bulbus (B).

- 1. As the apical loop depolarizes from band crossover with two simultaneous wavefronts (from the descending and the ascending band) it generates their synchronized contraction.
- 2. The activation of the ascending band propagates from

band crossover in two opposite directions: towards the apex and towards the base (Figure 4). The resulting mechanical contraction will also have a divergent direction, giving origin to the clockwise (apex) and counterclockwise (basal) rotations.

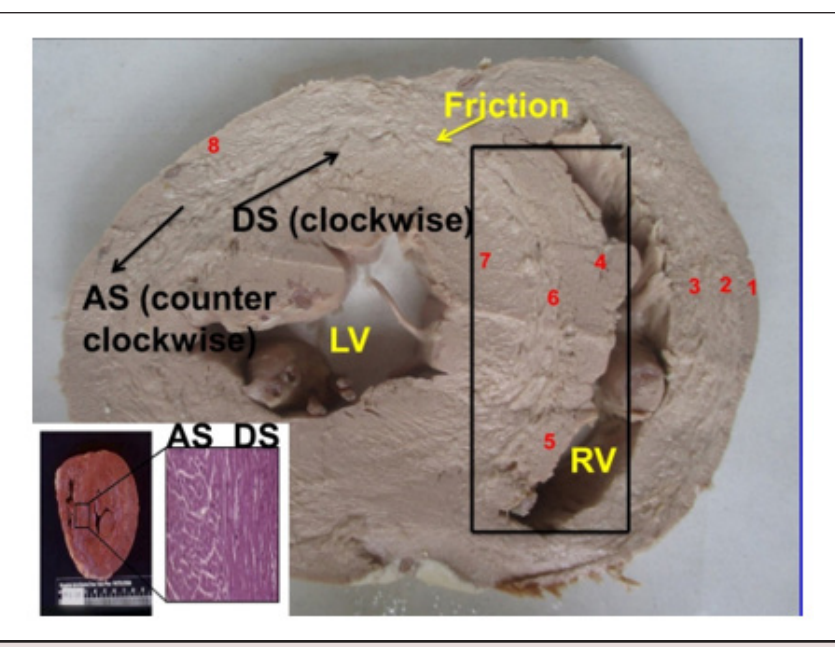
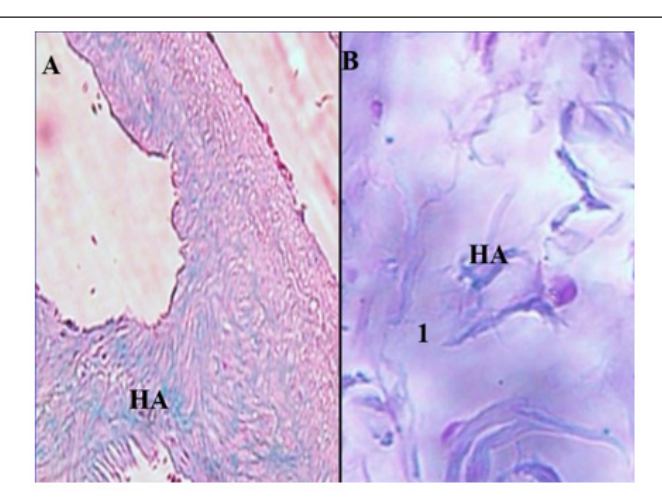
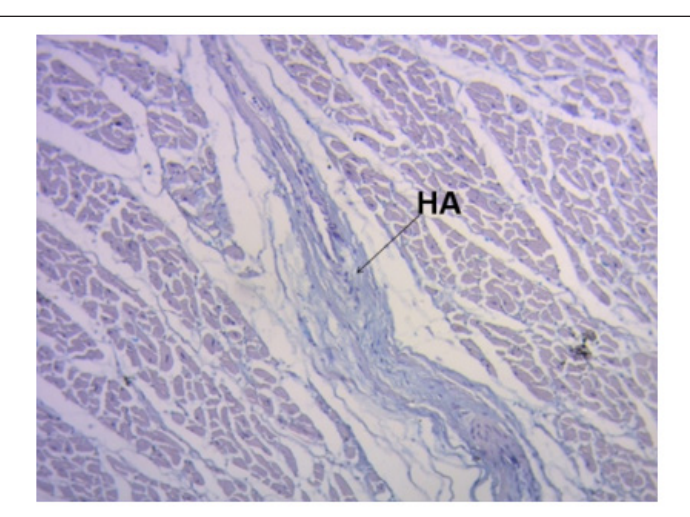


Figure 8: Cross-section of both ventricles (Human heart). References: 1. Interband fibers; 2. Right paraepicardial bundle; 3. Right paraendocardial bundle; 4. Anterior septal band; 5. Posterior septal band; 6. Intraseptal band; 7. Descending segment; 8. Ascending segment. The black arrows indicate the direction of movement of each segment in systole. The yellow arrow points to the plane of friction between both segments; counterclockwise (levogirous); clockwise (dextrogirous. The box shows the septum with the different segments that form it. In the lower corner, a microscopic view (right) of the interventricular septum middle segment in the human heart can be seen, clearly showing the absence of circumferential transition fibers between the fibers of the descending (right) and ascending (left) segments of the continuous myocardium. Also note how there is no fascia or anatomical structure interspersed between the two fiber bundles. Similarly, the macroscopic section (left), shows how the abrupt transition of the fiber angle change draws a line that can be seen with the naked eye and, in echocardiographic images, gives rise to the well-known midseptal linear image, generated by the acoustic interface that generates the abrupt change in angle in this area of the septum.



**Figure 9:** Histology of anuran (*Rhinella arenarum*) myocardium stained with Alcian Blue. A: 10x magnification; B: 40x magnification. Ref. 1: cardiomyocytes; HA: hyaluronic acid.



**Figure 10:** Contracted transverse vein with Alcian blue-positive edematous perivenous interstitium. Note the Alcian blue-stained Hyaluronic Acid (HA) in the interstitium between the cardiomyocytes (15x) (bovine heart).

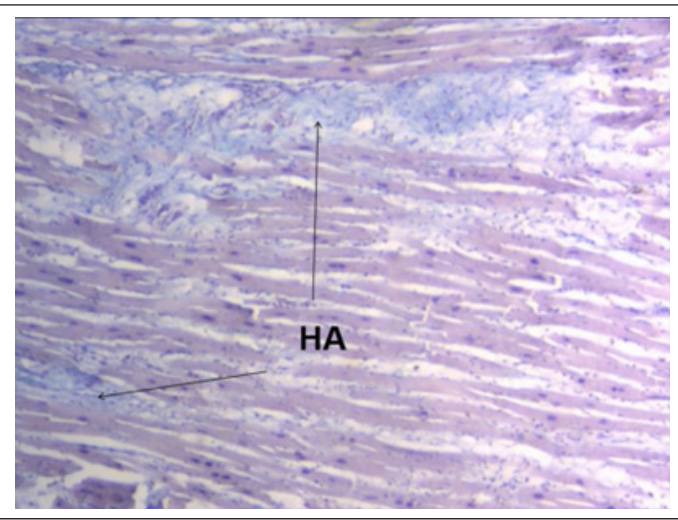


Figure 11: Interstitium between cardiomyocytes showing Hyaluronic Acid (HA) stained light blue with Alcian blue (15x) (adult human heart).

The helical myocardial arrangement forces the muscle to overlap segments in its spatial configuration. According to the electrophysiological studies we performed, this anatomical situation has great correspondence with myocardial movements and the stimulation that runs along its segments [26]. In a cardiac cross-section (Figure 8) below the atrioventricular valves, we can observe that the descending segment is located internally surrounded by the ascending segment in the free wall of the left ventricle [27]. The ascending and descending segments undergo opposite movements, both in systole and diastole, to achieve the expulsion and suction of ventricular blood contents, generating friction between their surfaces, a topic we have discussed in other publications when finding hyaluronic acid, with a lubricating function, in abundance both in the myocardium and in the Thebesius vessels in studies performed in anurans, bovines and humans (Figures 9 to 11) [28,29]. The histology in the box of Figure 8 clearly shows the different orientation of the fibers of the descending segment in relation to the ascending segment, which explains the opposite movements they present. The arrangement of myocardial fibers in the epicardium and endocardium, whose 180° angulation change causes the epicardial fibers to be arranged in the opposite orientation to the endocardial ones. Given the different anisotropic orientations of the fibers, this area corresponds to the beginning of the opposite movement that produces myocardial torsion. The constitution of the septum with the contiguity between the descending and ascending segments allows the continuity of activation between them with opposite move-

ments and the consequent myocardial torsion. The interventricular septum has a predominant value in the function of the myocardium since its location is essential in biventricular interdependence [30].

An important detail derived from tractographic images is their correspondence with the changes in angulation observed in the two-dimensional sections published by Streeter or with the rough arrangement of the band bundles in the anatomical sections of the recomposed hearts once dissected, highlighting the abrupt change in angulation present in the interventricular septum, due to the absence of transition of fibers with a circumferential course, since the septum is a structure that results from the apposition of the descending and ascending segments of the continuous myocardium [31].

The research aspect on the stimulation sequence allowed to determine the electrophysiological propagation in the continuous myocardium and also led to deductions about ventricular torsion and the suction effect in LVPPMC [32]. The orientation of the fibers in the continuous myocardium and its activation imply a concatenation of muscular movements in cardiac mechanics. These occur giving rise to four phases: narrowing, shortening-torsion, lengthening-detorsion and widening, which allow it to perform its functions of systole, suction and diastole. The fundamental movements in which the different segments of the continuous myocardium participate in systole and suction are shown in Table 4.

Table 4: Segment function.

Segment	Movement		
Right	Narrowing (systole)		
Left	Narrowing (systole)		
Descending	Shortening-torsion (systole)		
Ascending	Shortening-torsion (systole)		
Ascending (terminal portion)	Lengthening-detorsion (PPMC)		

This sequential activation correlates with fundamental phenomena that are well known today, such as the opposing clockwise and counterclockwise torsion of the apex and base of the left ventricle, which are responsible for its mechanical efficiency. In order to try to explain the mechanism of the muscular torsion, this research aimed to analyze the sequence of ventricular electrical activation by means of the simultaneous endo-epicardial MET of the segments from their beginning in the anatomical and functional contiguity between the AV node and the cardiac fulcrum (Figure 12).

In the narrowing phase there is a consecutive contraction of the right (free wall of the right ventricle) and left (edge of the mitral orifice) segments, which constitute the basal loop. According to Armour (1970) [33], this contraction constitutes an external cover within which the apical loop will contract. In reality, the crescentic

free wall of the right ventricle is located "ad latere" of the rest of the ventricular mass (septum and left ventricle), since the left segment constitutes part of the posterior epicardial wall of the left ventricle in its upper portion, surrounding the mitral annulus, while the rest of it is covered externally by the ascending segment. In this layer (basal loop) the stimulation goes from subepicardium to subendocardium. Then, it stimulates the descending segment and at 25.8 ms average in our research the ascending segment is activated. The end of the stimulation in the myocardium occurs at the level of the terminal part of the ascending segment, close to its insertion into the cardiac fulcrum, during the first 80-100 ms of diastole in the Protodiastolic Phase of Myocardial Contraction (PPMC) [34].

Since Harvey and later with Einthoven's electrocardiography, both the electrical activation and mechanical contraction of the

heart were considered to be linear and homogeneous processes. Thus, contraction would occur "en bloc" during systole and relaxation would occur uniformly during diastole. At this stage of current knowledge of the helical myocardium, these concepts do not

explain cardiac function, whose movements are sequential [35]. In this regard, the same occurs with cellular stimulation, which is explained in the diagram in Figure 13.

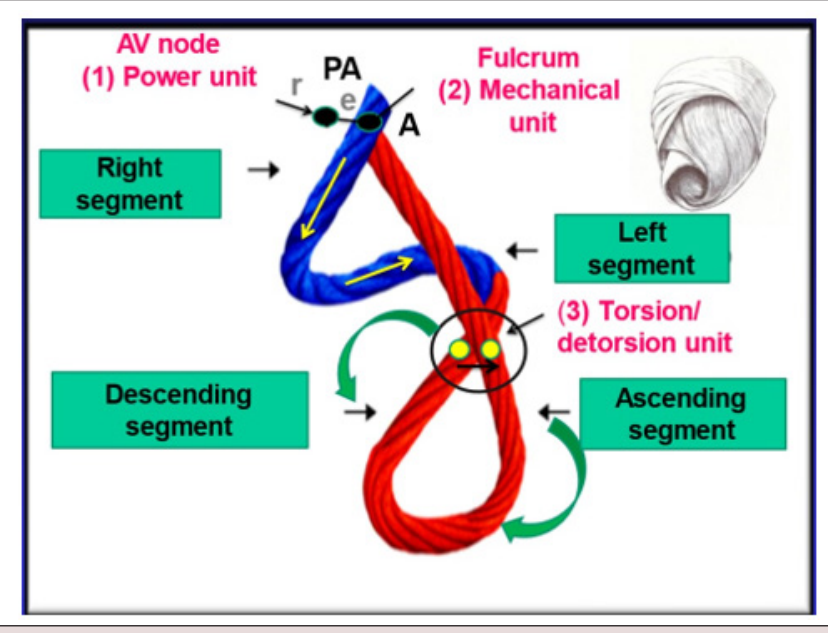
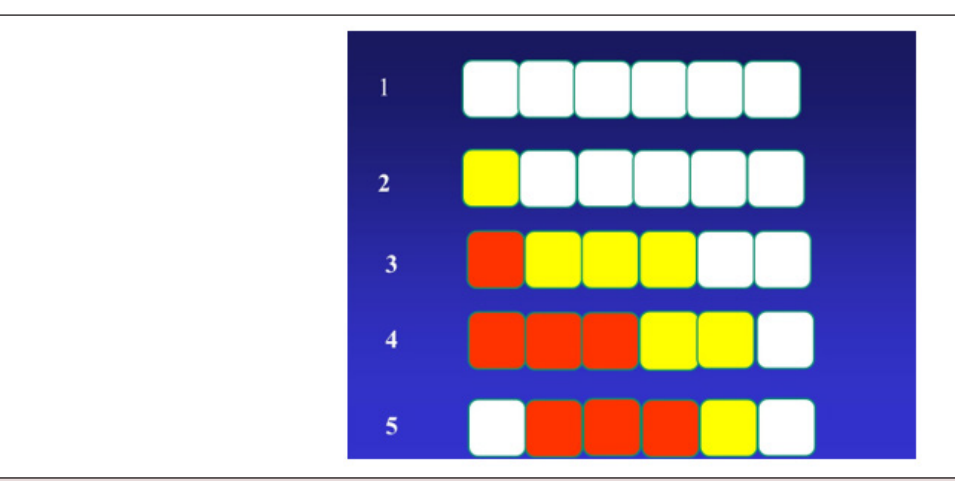


Figure 12: Helical myocardium in the cord model that simplifies the spatial structure. It shows the different segments that comprise it. In blue: basal loop. In red: apical loop. PA: pulmonary artery; A: Aorta; r: stimulus reception; e: stimulus emission. The three anatomical and functional units that allow integration between the AV node, the cardiac fulcrum, and myocardial torsion are detailed. The black circle details the site we have called band crossover. Given the different anisotropic orientations of the fibers, this area corresponds to the beginning of the helical opposite movement that produces myocardial torsion. The spatial arrangement of the continuous myocardium can be seen in the upper corner.



Note\*: White: excitable cell

Yellow: cell with stimulus conduction.

Red: cell in a refractory state.

Line 1: Cells in a state of excitability

Line 2: a cell initiates stimulus conduction

Line 3: the stimulus propagates to neighboring cells, leaving the initial cell in a refractory state

Line 4: the stimulation propagates through contiguity with other cells.

Line 5: After a certain time, the first cell to conduct becomes excitable again.

**Figure 13:** We have already analyzed that the myocardium contracts sequentially and not in a block manner. This stepwise propagation through its segments is repeated at the cellular level. Thus, the figure shows that excitable cells are then activated and subsequently become refractory, while cells that were in this last state become excited again to transmit the stimulus.

Although various aspects of electrical stimulus propagation in the ventricle have long been understood, the advent of three-dimensional navigators and electroanatomical mapping has enabled a much more detailed study of this process in the human heart under completely physiological clinical situations. This research allows us to elucidate the activation sequence of contractile areas and their entry into cardiac dynamics in relation to the path of the excitation wave with a coordinated pattern consistent with the helical structure of the continuous myocardium. Research conducted with MET explains the torsion phase of the heart, defined as the opposing rotational movement of the base and apex. Activation, for this purpose, at the intersection of the descending and ascending segments propagates from the endocardium to the epicardium (transverse propagation), that is, from the descending segment to the ascending segment.

This research on the transmission of impulses through the myocardium led to the investigations presented here, which correlate the structure of the continuous and helical myocardium with the propagation of stimulation. Our analysis implies that diffusion occurs simultaneously longitudinally and transversely between the descending and ascending segments. We must find a relationship between the activation action and the mechanical product. The explanation is provided by the simultaneous longitudinal and transverse electrical conduction pathways.

The ventricular narrowing phase (systolic isovolumic) at the beginning of systole is produced by the contraction of the right and left segments of the basal loop. The superimposed shortening phase is due to the descent of the base, which occurs simultane-

ously with myocardial torsion. It originates longitudinally when the annulus contracts before the apex. The fact that the latter does not move is due to the mechanism of the base descending in systole and ascending in diastole. The pressure generated to expel the largest amount of blood at the beginning of ejection, in a period that occupies only 20% of the systolic phase, is made possible by the torsional movement.

Although there is a progression in electrical conduction along the continuous myocardium, this isolated activation does not explain the generation of a force capable of ejecting ventricular contents at a speed of 200 cm/s at low energy expenditure. What was found in this investigation: the transverse propagation from the descending segment to the ascending one plays a fundamental role in ventricular torsion, allowing opposing forces on its longitudinal axis to generate the intraventricular pressure necessary to achieve the abrupt expulsion of blood. In this way, a torsion mechanism similar to "wringing out a towel" would be produced, as described by Giovanni Borelli and Richard Lower [27].

# The Three Electromechanical Units of the Heart, Conclusions

During this investigation, in both human, bovine and porcine hearts, the histological study revealed that the fulcrum (myocardial support, the beginning and end of the continuous myocardium) is adjacent to the AV node, creating a space rich in neurofilament plexuses. A crucial finding is that neurofilaments also occupy the cardiac fulcrum, constituting an electromechanical unit [36,37] (Figures 14 to 17).

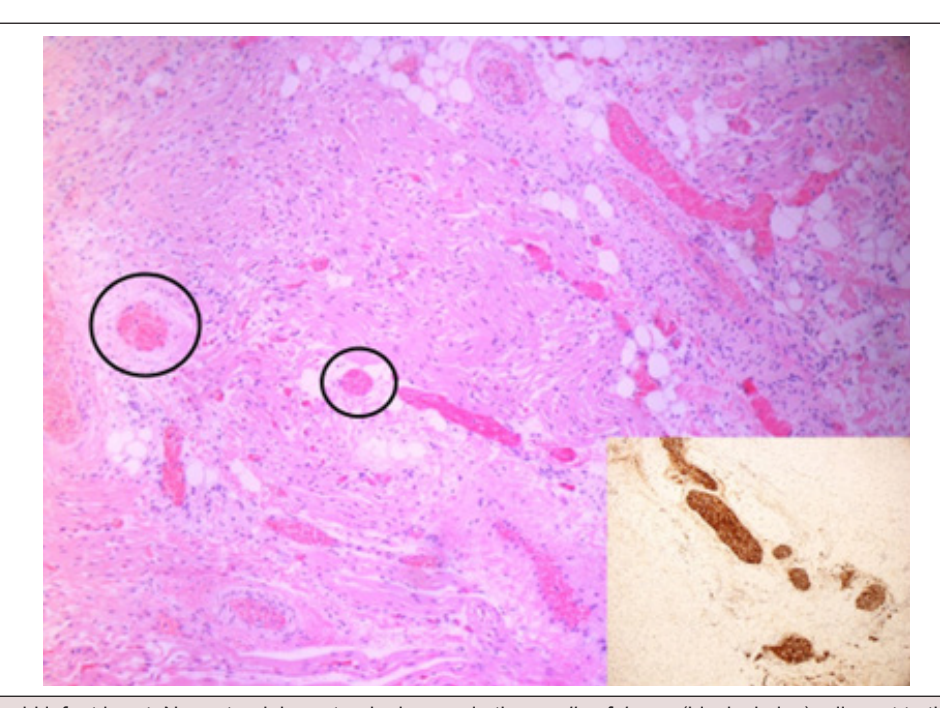


**Figure 14:** 27-week-old infant heart. Nerve trunk hypertrophy is seen in the *cardiac fulcrum* (black circles) adjacent to the AV node. HEx200. Inset shows thickened nerve trunk in the cardiac fulcrum confirmed by immunohistochemistry for S-100.

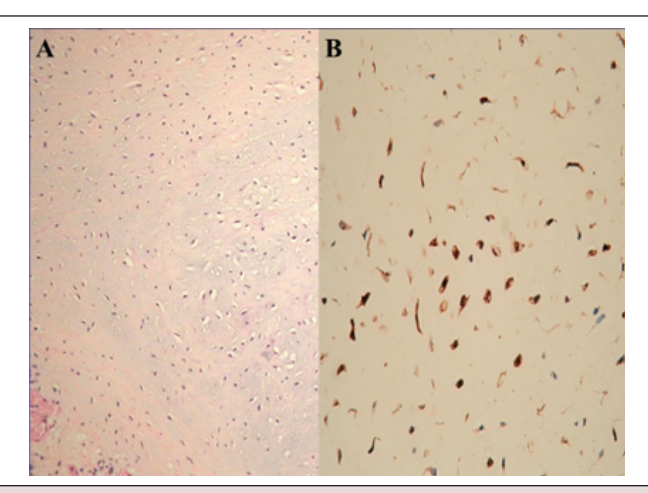


**Figure 15:** A 3-day-old premature neonate born at 27 weeks. Histological examination shows neurofilaments in the fulcrum adjacent to the atrioventricular node in A (A&E x 100). This finding is confirmed in B at higher magnification (H&E x 200) (immunohistochemistry with S-100).

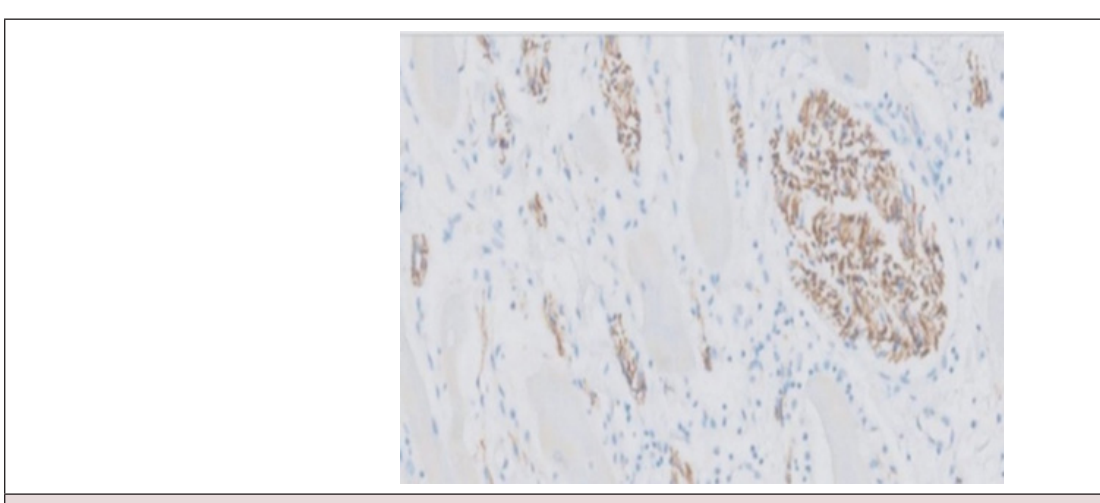


Figure 16: Porcine heart. Fulcrum-conduction cardiomyocytes with nerve plexuses in the spaces. Neurofilament stain (10x).

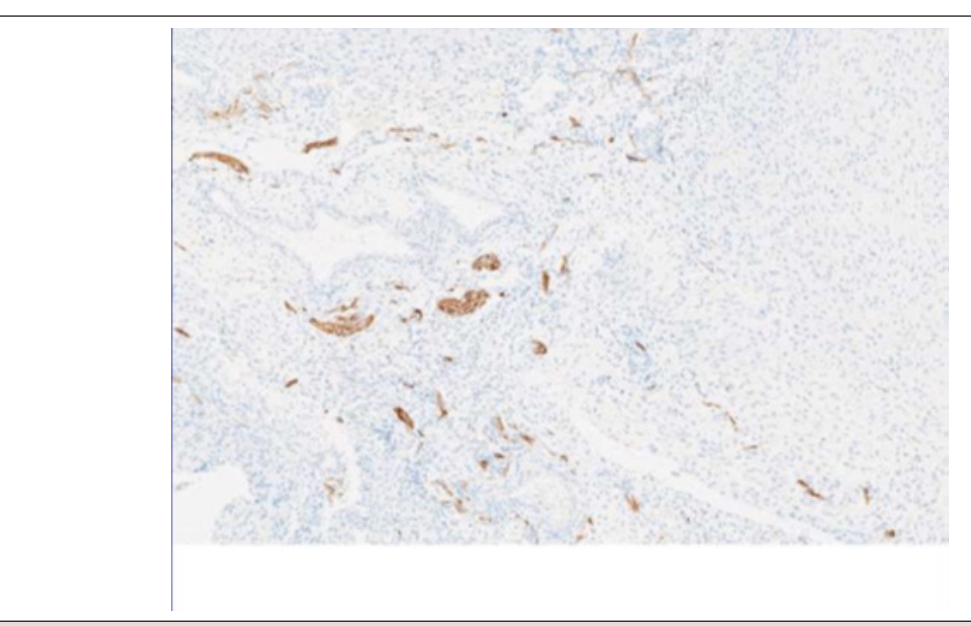


Figure 17: In the human heart, the neurofilament anchoring zone is shown in the fulcrum.

This contiguity between the two structures is found in all specimens studied (porcine, bovine and human hearts). Central to the research finding is that neurofilaments are also found within the cardiac fulcrum. Fibroblasts and connective tissue are located in the thickness of the conduction system and between this and the working myocardium, acting as an insulation layer. It is also the connective tissue that constitutes the fibrous ring and the central fibrocartilaginous portion of the fulcrum, thus electrically isolating the atrial and ventricular chambers [38-45]. We mapped left ventricular activation on its endocavitary and epicardial surfaces according to the methodology described above. The mapping was performed simultaneously with the surface ECG. This provided a unified temporal reference frame, allowing both recordings to be correlated and, on the one hand, to obtain a synchronized view of the simultaneous activation observed in various electroanatomical incidents.

This study found a relationship between myocardial stimulation and its mechanical product. The mechanical consequence of the cardiac structure is the initiation of stimulation in the anatomical and functional unit between the AV node and the cardiac fulcrum, and its continuity in myocardial activation up to the simultaneous activation zone with movements between the descending and ascending segments, which generates torsion of the myocardium, due to opposite rotation between the base and the apex, with simultaneous shortening of both ventricles.

In summary, cardiac movements are governed by three units (Figure 12):

- 1) Energy unit: Constituted by the AV node.
- 2) Electromechanical unit: Located at the cardiac fulcrum where the neurofilaments interact with the myocardium.
- 3) Torsion/detorsion unit: This occurs at the level where energy is transferred from the descending segment to the ascending segment, achieving myocardial torsion (systole) and the subsequent detorsion that allows ventricular suction.

### Acknowledgements

None.

### **Conflict of Interest**

None.

#### References

- 1. Bateson G (1979) Mind and nature: a necessary unity. Dutton, New York.
- Bertalanffy von L (1978) Teoría general de los sistemas. Alianza, Buenos Aires.
- Trainini J Trainini A. (2025) La Circulación de la Sangre. Ed. Biblos, Buenos Aires.
- Jason R Karamchandani, Torsten O Nielsen, Matt van de Rijn, Robert B West (2012) Sox10 and S100 in the diagnosis of soft-tissue neoplasms. Appl Immunohistochem. Mol Morphol 20: 445-450.

- Rushmer RF (1972) Structure and Function of the Cardiovascular System. Philadelphia, Saunders Company.
- Torrent Guasp F (1998) Estructura y función del corazón. Rev Esp Cardiol 51: 91-102.
- J Trainini, J Lowenstein, M Beraudo, M Wernicke, A Trainini, et al. (2021) Myocardial Torsion and Cardiac Fulcrum. J Morphol Anat 105(348): 15-23
- 8. Trainini J, Lowenstein J, Beraudo M, Mora Llabata V, Carreras Costa F, et al. (2022) El corazón helicoidal. Fulcro y Torsion. UNDAV Ed, Buenos Aires Argentina.
- Best A, Egerbacher M, Swaine S, Pérez W, Alibhai A, et al. (2022) Anatomy, histology, development and functions of Ossa cordis: A review. Anat Histol Embryol 00: 1-13.
- 10. Buckberg GD, Coghlan HC, Torrent Guasp F (2001) The structure and function of the helical heart and its buttress wrapping. V. Anatomic and physiologic considerations in the healthy and failing heart. Sem Thorac Cardiovasc Surg 13: 358-385.
- 11. Cosín Aguilar J, Hernándiz Martínez A, Tuzón Segarra MT, Agüero Ramón Llin J, Torrent Guasp F, et al. (2009) Experimental study of the so-called isovolumetric relaxation phase of the left ventricle. Rev Esp Cardiol 62: 392-399.
- 12. Arvidsson M, Töger J, Carlsson M, Steding Ehrenborg K, Pedrizzetti G, et al. (2017) Left and right ventricular hemodynamic forces in healthy volunteers and elite athletes assessed with 4D flow magnetic resonance imaging. Am J Physiol Heart Circ Physiol 312: H314-H328.
- 13. Carreras F, Ballester M, Pujadas S, Leta R, Pons Lladó G, et al. (2006) Morphological and functional evidences of the helical heart from noninvasive cardiac imaging. Eur J Cardiothoracic Surg 29(Suppl1): S50-5.
- Henson RE, Song SK, Pastorek JS, Ackerman JH, Lorenz CH, et al. (2000)
   Left ventricular torsion is equal mice and humans. Am J Physiol Heart Circu Physiol 278: H1117-H1123.
- Maksuti E, Carlsson M, Arheden H, Kovács S, Broomé M, Ugander M, et al. (2017) Hydraulic forces contribute to left ventricular diastolic filling. Scientif reports 7: 43505.
- 16. Pedrizzetti G, Arvidsson PM, Töger J, Borgquist R, Domenichini F, et al. (2017) On estimating intraventricular hemodymamic forces from endocardial dynamics: A comparative study with 4D flow MRI. J Biomech 60: 203-210.
- 17. Poveda F, Gil D, Martí E, Andaluz A, Ballester M, et al. (2013) Estudio tractográfico de la anatomía helicoidal del miocardio ventricular mediante resonancia magnética por tensor de difusión. Rev Esp Cardiol 66: 782-790.
- 18. Trainini JC, Trainini A, Valle Cabezas J, Cabo J (2019) Left Ventricular Suction in Right Ventricular Dysfunction. EC Cardiology 6: 572-577.
- 19. Ballester M, Ferreira A, Carreras F (2008) The myocardial band. Heart Fail Clin 4: 261-272.
- 20. Vicente Mora, Ildefonso Roldán, Elena Romero, Assumpció Saurí, Diana Romero, et al. (2018) Myocardial contraction during the diastolic isovolumetric period: analysis of longitudinal strain by means of speckle tracking echocardiography. J Cardiovasc Dev Dis 5: 41.
- 21. Vicente Mora, Ildefonso Roldán, Javier Bertolín, Valentina Faga, María Del Mar Pérez Gil, et al. (2021) Influence of ventricular wringing in the preservation of left ventricle ejection fraction in cardiac amyloidosis. J Am Soc Echocardiog 34: 767-774.
- 22. Torrent Guasp F, Buckberg G, Carmine C, Cox J, Coghlan H, et al. (2001) The structure and function of the helical heart and its buttress wrapping. I. The normal macroscopic structure of the heart. Seminars in Thorac and Cardiovasc Surg 13: 301-319.

23. Trainini JC, Beraudo M, Wernicke M, Carreras Costa F, Trainini A, et al. (2022) Evidence that the myocardium is a continuous helical muscle with one insertion. REC: CardioClinics 57: 194-202.

- 24. Sosa E, Scanavacca M, d Avila A, Pilleggi F (1996) A new technique to perform epicardial mapping in the electrophysiology laboratory. J Cardiovasc Electrophysiol 7: 531-6.
- Trainini J (2024) In Search of the Cardiac Fulcrum. The finding of the support of the heart. Ed. Biblos, Buenos Aires, Argentina.
- 26. Valle J, Herreros J, Trainini J, García Jimenez E, Talents M, et al. (2017) Three-dimensional definition of Torrent Guasp's ventricular muscle band and its correlation with electric activation of the left ventricle (abstract). XXIII Congreso SEIQ, Madrid, España 105: 2.
- 27. Trainini J, Lowenstein J, Beraudo M, Valle Cabezas J, Wernicke M, et al. (2023) Anatomy and organization of the helical heart. UNDAV Ed., Buenos Aires.
- 28. Trainini JC, Wernicke M, Beraudo M, Lowenstein J, Trainini A, et al. (2021) Hyaluronic acid in the heart. J Trends Biomedical Research 4: 1.
- 29. Trainini J, Beraudo M, Wernicke M, Carreras Costa F, Trainini A, et al. (2022) The hyaluronic acid in intramyocardial sliding. REC: CardioClinics 2022.
- Rodríguez Padilla J, Petras A, Magat J, Bayer J, Bihan Poudec Y, et al. (2022) Impact of intraventricular septal fiber orientation on cardiac electromechanical function. Am J Physiol Heart Circ Physiol 322: H936-H952.
- 31. Torrent Guasp F (1987) Nuevos conceptos sobre la estructura miocárdica ventricular. En Torrent Guasp F, editor. Estructura y mecánica del corazón. Barcelona: Grass Ed 35-97.
- 32. Trainini JC, Lowenstein J, Beraudo M, Trainini A, Mora Llabata V, et al. (2019) Myocardial Torsion. Ed Biblos, Buenos Aires; Argentina.
- 33. Armour JA, Randall WC (1970) Structural basis for cardiac function. Am J Physiol 218: 1517-1523.
- 34. Trainini J, Lowenstein J, Beraudo M, Wernicke M, Mora Llabata V, et al. (2022) Cardiac Helical Function. Fulcrum and Torsion. Japan Journal of Clinical & Medical Research SRC/JJCMR-139.

- 35. Ballester Rodés MA, Flotats A, Torrent Guasp F, Carrió Gasset I, Ballester Alomar M, et al. (2006) The sequence of regional ventricular motion. Eur J Cardiothorac Surg 29: 139-144.
- 36. Trainini J, Wernicke M, Beraudo M, Cohen M, Trainini A, et al. (2023) Cardiac Fulcrum, its Relationship with the Atrioventricular Node. Rev Argent Cardiol 91: 429-435.
- 37. Trainini Jorge, Beraudo Mario, Wernicke Mario, Trainini Alejandro, Lowenstein Jorge, et al. (2024) Fundamental Conclusions on Research into the Anatomy and Organization of the Helical Heart. Am J Biomed Sci & Res 23(5).
- 38. Sosa Olavarría A, Martí Peña A, Martínez A, Zambrana Camacho J, Ulloa Virgen J, et al. (2023) Fulcro cardíaco de Trainini en el corazón fetal. Rev Peru Ginecol Obstet 69(4): 1-8.
- 39. Trainini JC, Mora V, Lowenstein J, Beraudo M, Wernicke M, et al. (2020) La teoria de la banda miocárdica Nuevos descubrimientos que apoyan el complejo mecanismo de torsión miocárdica. Revista de Ecocardiografía Práctica y Otras Técnicas de Imagen Cardíaca 3: 14-18.
- 40. Trainini J, Wernicke M, Beraudo M, Trainini A (2024) The Fulcrum of the Human Heart (Cardiac fulcrum). J Cardiol Cardiovasc Med 9: 001-005.
- 41. Trainini J, Wernicke M, Beraudo M, Trainini A (2024) The fulcrum of the human heart (Cardiac fulcrum). World Journal of Biology Pharmacy and Health Sciences 17(01): 049-056.
- 42. Trainini Jorge, Beraudo Mario, Wernicke Mario, Efraín Herrero, Trainini Alejandro (2024) The Cardiac Fulcrum-Comments. AJ Biomed Sci & Res 23(4).
- 43. Trainini J, Beraudo M, Wernicke M, Herrero E, Trainini A (2024), The Cardiac Fulcrum Comments. International Journal of Cardiovascular Medicine 3:5.
- 44. Trainini J, Beraudo M, Wernicke M, Herrero E, Trainini A, (2025) Propiedades del Fulcro Cardíaco. Rev Argent Cardiol 93: 43-49.
- 45. Trainini J, Beraudo M, Wernicke M, Freire G, Trainini A, et al. (2025) Helical Heart Suction in Heart Failure with Preserved Ejection Fraction. Am J Biomed Sci & Res 25(6).